REVIEW OF PRECISION DETERMINATIONS OF THE ACCELERATOR LUMINOSITY IN LEP EXPERIMENTS *

G.M. DALLAVALLE
I.N.F.N., Dipartimento di Fisica dell'Universitá
Bologna, Italy

(Received January 14, 1997)

The LEP collaborations ALEPH, DELPHI, L3 and OPAL were able to measure the accelerator luminosity with an experimental uncertainty smaller than 0.1%. Motivations, method, technological aspects and main difficulties of the measurements are reviewed.

PACS numbers: 07.90. +c

In the years from 1992 to 1994 the LEP collaborations ALEPH, DELPHI, L3 and OPAL have upgraded their luminosity monitors (references [1] to [11]). The aim was a luminosity measurement at the 0.1% level, in order to make optimal use of the high statistics of Z delivered at LEP1.

The cross section σ_X for a process $e^+e^- \to Z \to X$ at LEP1 is obtained by normalizing the number of observed events N_X to the total luminosity L available for the detector: $\sigma_X = N_X/L$. In general, when the sample of Z decays N_X becomes larger than 10^6 events, the uncertainty on L has to be smaller than 0.1%, otherwise it becomes the limiting factor in measuring σ_X. More specific requirements on the luminosity uncertainty, which take into account both statistical and systematic errors, are set by analyzing how the $\Delta L/L$ error propagates in the uncertainty on the Z lineshape parameters measured at LEP1, in particular on $\Gamma_{\rm inv}/\Gamma_{\rm lept}$ and on $\Gamma_{\rm lept}$.

In the Standard Model the ratio $\Gamma_{\rm inv}/\Gamma_{\rm lept}$ of the Z width in invisible decays to the Z width in leptonic decays is calculated very accurately, with a residual uncertainty of 0.05% due to the uncertainty on the top and Higgs masses ($m_t = 175 \pm 6$ GeV [12], $60 < m_{\rm H} < 1000$ GeV). The measurement of

* Presented at the Cracow International Symposium on Radiative Corrections to the Standard Model, Cracow, Poland, August 1-5, 1996.

$\Gamma_{\rm inv}/\Gamma_{\rm lept}$ is therefore a strong test of the Standard Model. Experimentally $\Gamma_{\rm inv}/\Gamma_{\rm lept}$ is calculated via the relation

$$\frac{\Gamma_{\rm inv}}{\Gamma_{\rm lept}} = \frac{\Gamma_Z - \Gamma_{\rm had} - 3\Gamma_{\rm lept}}{\Gamma_{\rm lept}}, \tag{1}$$

where Γ_Z is the Z total width and $\Gamma_{\rm had}$ is the Z width in hadronic decays. Equation (1) can be rewritten as

$$\frac{\Gamma_{\rm inv}}{\Gamma_{\rm lept}} = \left(\frac{12\pi}{M_Z^2}\right)^{1/2} \left(\sigma^0_{\rm lept}\right)^{-1/2} - R_l - 3, \tag{2}$$

where the experimentally accessible quantities M_Z, $\sigma^0_{\rm lept}$ (cross section for $e^+e^- \to Z^0 \to l\bar{l}$ at the Z pole) and $R_l = \Gamma_{\rm had}/\Gamma_{\rm lept}$ appear explicitly. The uncertainty on $\Gamma_{\rm inv}/\Gamma_{\rm lept}$ has principal contributions from the uncertainties on the hadronic and leptonic decays of the Z and from $\Delta L/L$:

$$\Delta\frac{\Gamma_{\rm inv}}{\Gamma_{\rm lept}} = 6\frac{\Delta N_{\rm lept}}{N_{\rm lept}} \oplus 21\frac{\Delta N_{\rm had}}{N_{\rm had}} \oplus 15\frac{\Delta L}{L}. \tag{3}$$

In Fig. 1 the contribution to $\Delta\Gamma_{\rm inv}/\Gamma_{\rm lept}$ due to the statistical and systematic errors on $N_{\rm had}$ and $N_{\rm lept}$ is plotted for an increasing number of collected Z decays and it is compared to the contribution due to $\Delta L/L$. The systematic errors are assumed to improve according to a realistic pattern. Clearly, with the large sample of a few times 10^6 events which, back in 1991, each one of the four LEP collaborations expected in the years to come, the target had to be a $\Delta L/L$ error at the 0.1% level. The current sample of Z decays consists of more than 4×10^6 events per LEP experiment [13].

A $\Delta L/L$ error at the 0.1% level also optimizes the extraction of the so called "derived quantities" in the lineshape measurement at LEP1. Let us consider the Z width $\Gamma_{\rm lept}$ in leptonic decays. $\Gamma_{\rm lept}$ is strongly sensitive to m_t through radiative corrections and it has no dependence on α_s. The experimental uncertainty on $\Gamma_{\rm lept}$ can be expressed as

$$\frac{\Delta\Gamma_{\rm lept}}{\Gamma_{\rm lept}} = \frac{\Delta\Gamma_Z}{\Gamma_Z} \oplus \frac{1}{2}\left(\frac{\Delta N_{\rm lept}}{N_{\rm lept}} \oplus \frac{\Delta L}{L}\right). \tag{4}$$

In Fig. 2 the theoretical prediction for $\Gamma_{\rm lept}$ is plotted as function of m_t for $60 < m_{\rm H} < 1000$ GeV using ZFITTER [14]. Two bands, representing the LEP current measurement of $\Gamma_{\rm lept}$ [13] and the m_t current measurement at the Tevatron [12], are superimposed to the plot. The points on a side are used to indicate what the LEP error band would be for different values of the $\Delta L/L$ error.

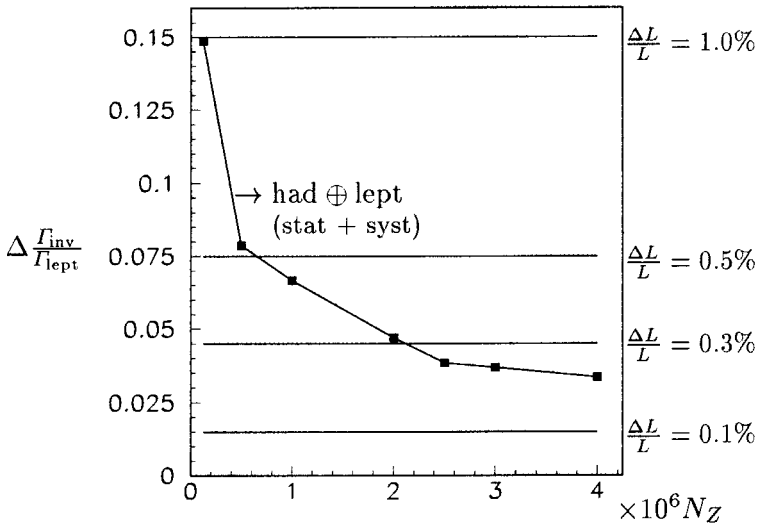

Fig. 1.

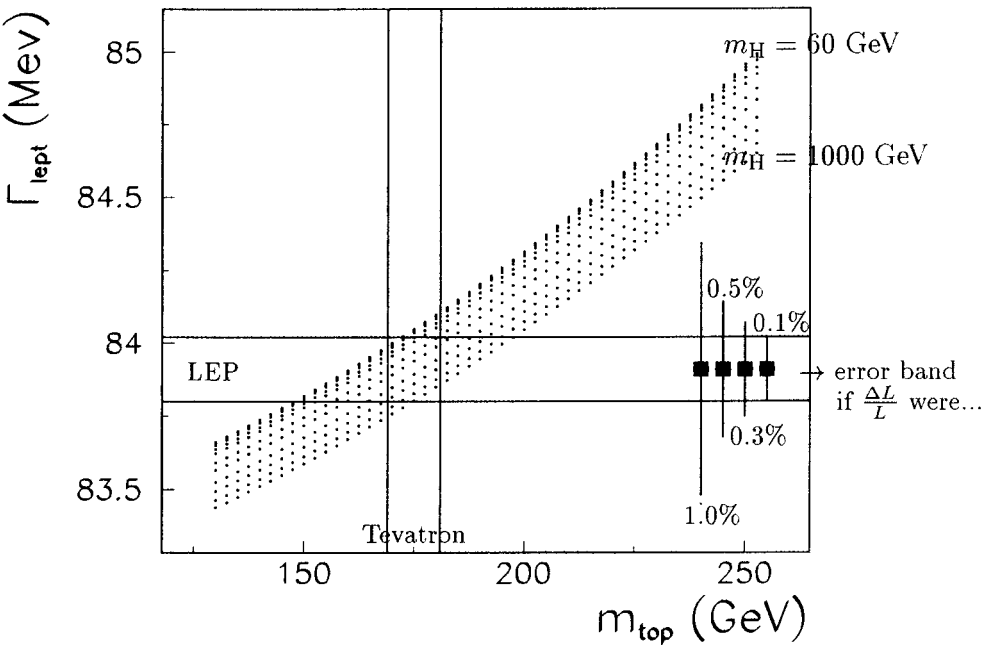

Fig. 2.

At LEP, the accelerator luminosity L is measured via the relation $L = N_{\rm Bh}/\sigma_{\rm Bh}$, in which $N_{\rm Bh}$ is the number of small-angle $e^+e^- \to e^+e^-$ (Bhabha

scattering) events detected in a fiducial acceptance, and σ_{Bh} is the theoretical Bhabha cross section in that fiducial acceptance. The motivation is twofold:

- small-angle Bhabha scattering is a QED process, t-channel dominated, which means that (a) σ_{Bh} is calculable with high precision (currently the theoretical uncertainty is 0.11%, see [15] and [16], when using the BHLUMI event generator [17]) and (b) interference with Z production in the s-channel is small (small impact on the Z lineshape measurement at LEP1);
- σ_{Bh} is large, which means that (a) the statistical uncertainty in the L measurement is small and (b) there is no statistical limitation in studying the experimental systematics.

In order to maximize the benefit, the detection angular region is as close as possible to the beam line.

Small-angle Bhabha events are detected as signal coincidences of the forward luminometer with the backward luminometer. A typical selection of fiducial "luminosity" Bhabha events in the LEP experiments has (see sketch in Fig. 3):

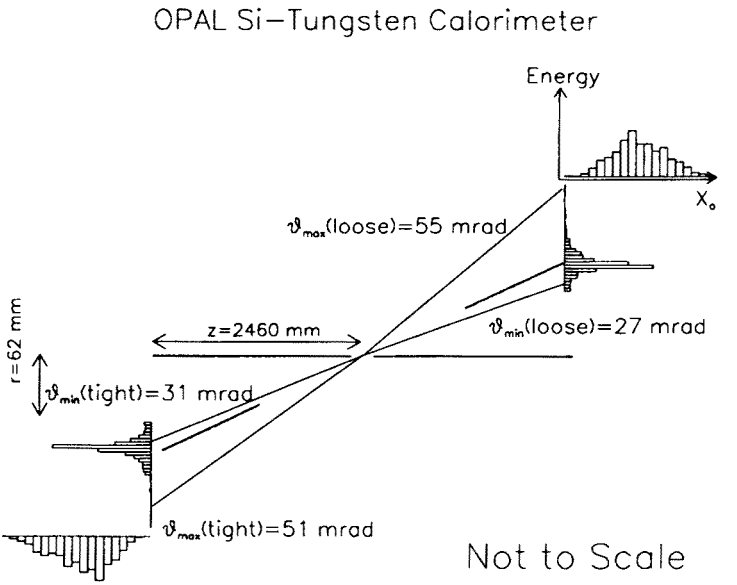

Fig. 3.

- an **asymmetric** angular acceptance, for instance a narrower (N) acceptance in the luminometer on the e^+ side and a wider (W) acceptance

on the e^- side. The NW and WN selections run concurrently; the two results are averaged. The aim is to minimize the dependence on the interaction point (IP) position and on the beam tilt. As a by-product, also events with photon radiation are accepted in which the radiated photons remain undetected inside the beam pipe (mainly "initial state" radiation).

- a **calorimetric** measurement of the scattered e^+ and e^-. The aim is to minimize the dependence on the material in front of the luminometer, causing preshowering. As a by-product, also events with photon radiation are accepted in which the radiated photons are close to the scattered electrons (mainly "final state" radiation).
- very mild energy and/or acollinearity cuts on the scattered e^+ and e^-, compatible with the previous two items.

Inclusion of radiative events is ultimately a big advantage when calculating the total cross section σ_{Bh} in the fiducial acceptance, because it reduces the sensitivity to the differential distributions of the radiated photons which differ from calculation to calculation. This is shown in Tables I, II (from [15])

TABLE I

BHL − OB		*Acollinearity cut (rad)*		
		0.005	0.010	no cut
x_{min}^{cut}	0.999	11.35(1)%	10.86(1)%	10.61(1)%
	0.99	4.65(1)%	4.45(1)%	4.35(1)%
	0.90	0.69(2)%	0.60(1)%	0.58(1)%
	0.85	0.68(1)%	0.25(1)%	0.24(1)%
	0.75	0.75(1)%	0.12(1)%	-0.00(1)%
	triangular	0.78(1)%	0.16(1)%	-0.09(1)%
	0.50	0.83(1)%	0.26(1)%	0.06(1)%

which compare the results of the BHLUMI and OLDBIS calculations [17]. BHLUMI is a Monte Carlo event generator for Bhabha scattering with multi-photon radiation based on an exponentiated $O(\alpha^2)$ calculation. OLDBIS is a Monte Carlo event generator for Bhabha scattering with single-photon radiation based on an $O(\alpha)$ calculation; it is a revision of the BABAMC event generator [18]. TABLE I reports the cross section difference BHLUMI - OLDBIS normalized to the BHLUMI cross section for the RSA Bhabha event selection of [15] ($x = E_{\text{cluster}}/E_{\text{beam}}$). The label "triangular" stands for the cut $0.5(x_{e+} + x_{e-}) > 0.75$. Table II reports the relative variation of the accepted Bhabha cross section with respect to the RSA Bhabha event selection

TABLE II

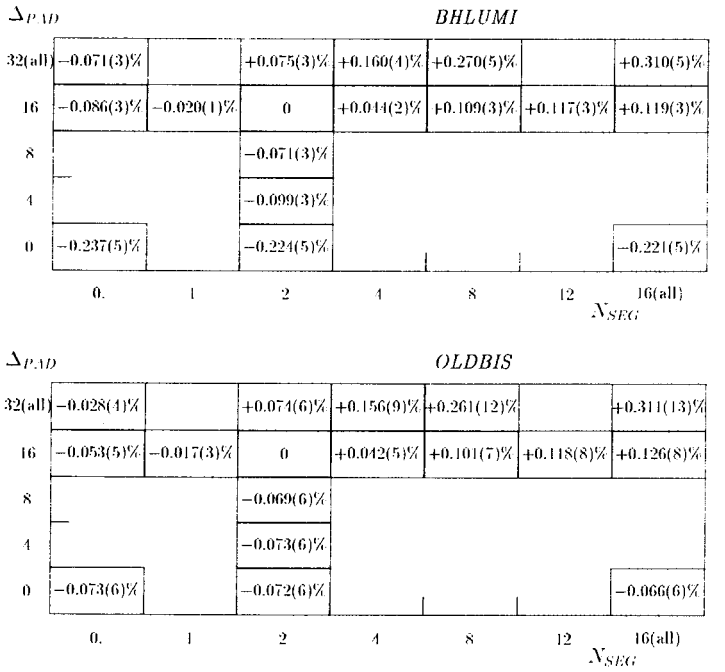

of [15] when changing cluster radial (PADs) and azimuthal (SEGments) dimensions. A cluster extends for $\pm\Delta_{\text{PAD}}$ pads and $\pm N_{\text{SEG}}$ segments around the pad containing the largest energy deposit. A pad is assumed to subtend a polar angle of about 1 mrad; a segment covers azimuthally an angle of 11.25 degrees. The RSA selection has $\Delta_{\text{PAD}} = 16$ and $N_{\text{SEG}} = 2$. In [15] it is concluded that large cluster sizes, rather soft energy cuts and an asymmetric (Wide–Narrow) acceptance are very effective in minimizing the cross section difference BHLUMI-OLDBIS.

In the LEP experiments the basic element of a luminometer is an electromagnetic calorimeter with cylindrical symmetry about the beam axis. The inner radius $R_{\min}$ of the detector is limited by the beam pipe. Major experimental systematic errors on the L measurement potentially come from:

- ALIGNMENT: poor knowledge of the detector internal geometry and alignment. The Bhabha cross section has a steep angular dependence

$$\sigma_{\mathrm{Bh}} = k\left(\frac{1}{\theta^2_{\min}} - \frac{1}{\theta^2_{\max}}\right) = k\, Z_{\mathrm{det}}\left(\frac{1}{R^2_{\min}} - \frac{1}{R^2_{\max}}\right), \tag{5}$$

  where Z_{det} is the distance from the interaction region at which the luminometer is located along the beam line. Assuming $R_{\min} = 7$ cm, $R_{\max} = 14$ cm and $Z_{\mathrm{det}} = 2.5$ m (consistently with the LEP experiments), the relative uncertainties $\Delta L/L$ on the measured luminosity due to uncertainties on $R_{\min}$, $R_{\max}$ and Z_{det} are

$$\begin{aligned}
\frac{\Delta L}{L} &= \pm\frac{\Delta R_{\min}(\mu\mathrm{m})}{26(\mu\mathrm{m})}\ 10^{-3}, \\
\frac{\Delta L}{L} &= \mp\frac{\Delta R_{\max}(\mu\mathrm{m})}{210(\mu\mathrm{m})}\ 10^{-3}, \\
\frac{\Delta L}{L} &= \pm\frac{\Delta Z_{\mathrm{det}}(\mathrm{mm})}{1.25(\mathrm{mm})}\ 10^{-3}
\end{aligned} \tag{6}$$

  which directly show how much accurate the detector survey has to be for a luminosity measurement with $\Delta L/L = 0.1\%$.

- BEAM: poor knowledge of the beam parameters, in particular the IP position and the beam tilt. Displacements of the IP are both along the beam line and transverse to it. The $\Delta L/L$ variation due to a longitudinal displacement ΔZ of the IP is minimized when averaging the Narrow–Wide and the Wide–Narrow luminosity measurements:

$$\begin{aligned}
\frac{\Delta L}{L}(NW) &= -\frac{\Delta Z(\mathrm{mm})}{1.25(\mathrm{mm})}\ 10^{-3} + \left(\frac{\Delta Z(\mathrm{mm})}{79.1(\mathrm{mm})}\right)^2\ 10^{-3}, \\
\frac{\Delta L}{L}(WN) &= +\frac{\Delta Z(\mathrm{mm})}{1.25(\mathrm{mm})}\ 10^{-3} + \left(\frac{\Delta Z(\mathrm{mm})}{79.1(\mathrm{mm})}\right)^2\ 10^{-3}, \\
\frac{\Delta L}{L} &= \frac{1}{2}\left(\frac{\Delta L}{L}(NW) + \frac{\Delta L}{L}(WN)\right) = \left(\frac{\Delta Z(\mathrm{mm})}{79.1(\mathrm{mm})}\right)^2\ 10^{-3}
\end{aligned} \tag{7}$$

  which is practically negligible at LEP. A transverse displacement ΔX of the beam causes an eccentricity of the beam axis with respect to the

detector axis. Its effect on the accepted Bhabha cross section, when integrated in azimuth, cancels to first order but not to second order:

$$\frac{\Delta L}{L} = \left(\frac{\Delta X(\text{mm})}{1.5\ (\text{mm})}\right)^2 10^{-3}. \tag{8}$$

The beam eccentricities in the forward luminometer and in the backward luminometer can be different because of a beam tilt. The beam parameters are measured on a fill-by-fill basis during the data taking period and a correction is applied to the measured luminosity.

- BACKGROUND: background from accidental forward-backward coincidences of off-momentum beam electrons mimicking Bhabha events

The relevant features of the luminometers of the four LEP experiments are summarized in Table III. One should underline the great care which was put in the survey and alignment of the detectors. The luminosity uncertainty is smaller than 0.1% in all four experiments [3, 6, 8, 11]. In the following a few highlights from each one of the four measurements are discussed.

In the OPAL detector, luminosity Bhabha events are tagged by two small-angle calorimeters placed on opposite sides with respect to the IP. Each calorimeter [10] is a sandwich of tungsten plates for a total of 22 X_0 interleaved with 19 silicon detectors. The use of tungsten as absorber makes the calorimeter very compact and keeps the transverse size of the electron showers small. The first 14 X_0 are sampled every 1 X_0, the last 8 X_0 are sampled every 2 X_0. A silicon detector layer consists of 16 azimuthal wedges. Each wedge is a silicon pad detector (300 μm thick) with the pads arranged in two radial columns of 32 pads, as shown in Fig. 4. The pad width is 2.5 mm. The radial coordinate of impact of an electron on the detector front face is reconstructed from the positions of the shower centroids in 9 consecutive layers (from 2 to 11 X_0), in order to minimize the effect of inefficiencies and mismeasurements in single layers. The inner and outer radial fiducial acceptance cuts for luminosity Bhabha events are put on the radial coordinate in correspondence of pad boundaries in the silicon layer 7 X_0 deep in the calorimeter (close to the average shower maximum), f.i. the boundary between pads 6 and 7 for R_{min}. In Fig. 5 the distribution of the radii measured in Bhabha events is shown for events having maximum deposited energy above or below the pad 6/7 boundary in the layer at 7 X_0. Although the position of that pad boundary is known with high accuracy from the calorimeter survey, effects exist that can create biasses in the measured coordinate.

TABLE III

collaboration	L3	ALEPH	OPAL	DELPHI
technology	BGO calorimeter and Si Rϕ strips (3 planes)	Sandwich calorimeter Tungsten+Si pads (12 samplings)	Sandwich calorimeter Tungsten+Si pads (18 samplings)	Shashlik calorimeter Lead+Scintillator tiles (47 samplings)+Si pads (2 pl.) and veto counters
reference	CERN-PPE/96-89 sub.NIM A	N.I.M. A 365(1995)117	IEEE Trans. 41(1994)845	DELPHI note 95-68 PHYS 503
proposal	CERN/LEPC 92-6	CERN/LEPC 90-3	CERN/LEPC 91-8	CERN/LEPC 92-6
installation	1993	Sep.1992	1993	1994
Z from IP	2650 mm(Si) 2730 mm(BGO)	2503.2 mm(front) 2546.8 mm(fiducial)	2389 mm(front) 2460.2 mm(fiducial)	2200.6 mm(STIC)
$\Delta_{sys}Z$	0.4 mm	0.5 mm	0.08 mm	0.3 mm
detector $R_{min}//R_{Max}$	76. // 154. mm	61. // 144.5 mm	62. // 142. mm	65. // 420. mm
$\Delta_{sys}R_{min}$ alignment temperature effects	6 μm 5 μm	9 μm 3 μm	9 μm 3 μm	20 μm (17X_o Tungs. mask)
X_o in front of detector	0.05 // 0.5	0.54	0.3	0.51
$\theta_{min}//\theta_{Max}$ fiducial	32. // 54. mrad	30. // 48.5 mrad	31.3 // 51.6 mrad	43.6 // 113.6 mrad
σ_{Bhabha} in acceptance	69.62 nb	84.11 nb	78.81 nb	54.95 nb
Δ_{sys} of L measurement experimental M.C. statistics total	preliminary 0.05 % 0.06 % 0.078 %	preliminary 0.069 % 0.024 % 0.073 %	preliminary 0.065 % 0.037 % 0.075 %	preliminary 0.085 % 0.03 % 0.09 %

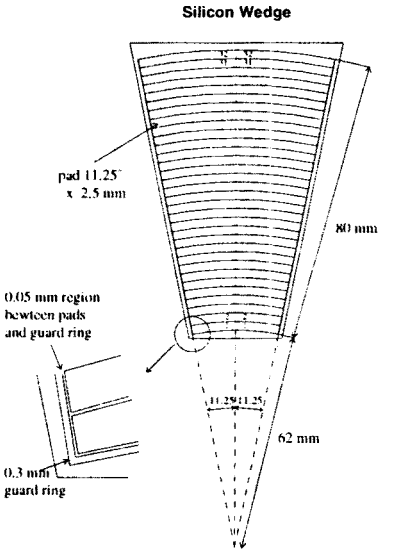

Fig. 4. OPAL

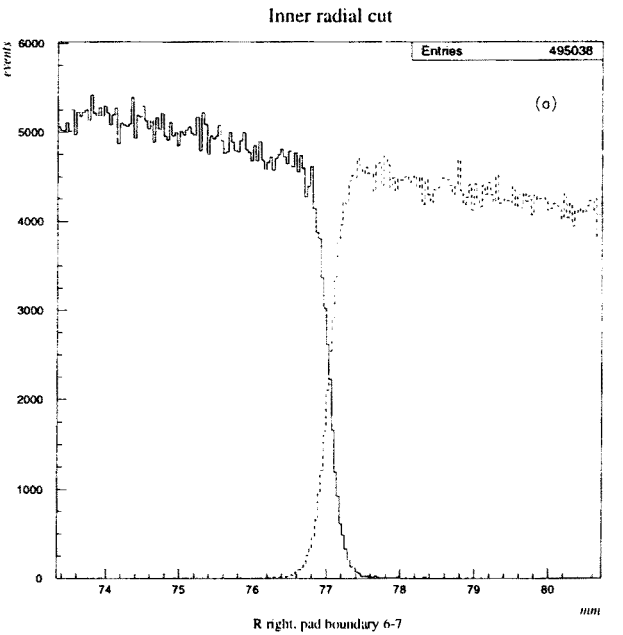

Fig. 5. OPAL

The thermal expansion of the detector (about 2 $\mu m/°C$) is controlled by maintaining the detector at quasi constant temperature during the data taking. One subtle effect is the bias due to the curvature of the pad boundaries coupled to the azimuthally increasing dimensions of the pads when moving radially out. The shower centroid in a layer is reconstructed from the energy deposits in contiguous pads and it appears to lie at the pad boundary when the energy deposits in the pads below and above the boundary are equal. The difference ΔR between true and reconstructed position of a pad boundary has been directly measured by comparing the reconstructed pad boundaries with an electron beam and with a muon beam : $\Delta R = 8 \pm 6\ \mu m$. The full list of experimental systematic errors in the OPAL luminosity measurement is reported in Table IV [11].

TABLE IV

OPAL preliminary [11]

This Table summarizes the corrections applied and the corresponding experimental systematic uncertainties on the absolute L_{RL} luminosity measurement. They are shown separately for the 1993 and 1994 measurements. The errors are decomposed into the components which are correlated amongst the 1993 and 1994 data sets, and those which are not.

	Correction $\times 10^{-4}$		Systematic $\times 10^{-4}$	
Effect on L_{RL}	1993	1994	1993	1994
SiW radial dimensions ($\pm 9 \mu m$)			3.6 ± 0.0	3.6 ± 2.0
Radial coordinate bias			3.3 ± 0.8	3.3 ± 0.5
Monte Carlo, detector response	-7.3	-7.3	3.8 ± 0.3	3.8 ± 0.3
Monte Carlo, statistics			3.7 ± 0.0	3.7 ± 0.0
Detector instability (mech. + response)			0.5 ± 0.0	0.5 ± 0.0
Trigger inefficiency	0	0	< 0.01	< 0.01
LEP Beam parameters (average)	$+3.1$	$+4.4$	1.9 ± 0.5	1.9 ± 0.4
Fluctuations in LEP beam parameters			0.0 ± 0.5	0.0 ± 0.5
Accidental coincidence background	$+1.0$	$+0.1$	0.0 ± 0.1	0.0 ± 1.0
$\gamma\gamma$ background	$+2.0$	$+2.0$	0.1 ± 0.0	0.1 ± 0.0
Total	-1.2	-0.8	7.5 ± 1.1	7.5 ± 2.4

Fig. 6 shows the Bhabha event distribution in radius for the data and for the BHLUMI Monte Carlo. The agreement is excellent.

In the DELPHI detector, luminosity Bhabha events are tagged by two small-angle calorimeters of the "shashlik" type placed on opposite sides of the IP. Each calorimeter (STIC) [5] has 27 X_0 of lead equipped with 47 layers of scintillator tiles. The tiles are read out in towers with projective geometry

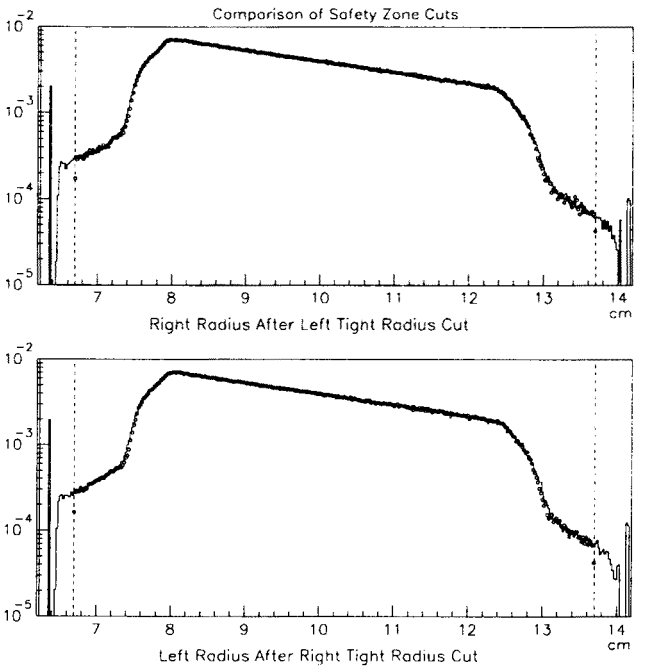

Fig. 6. OPAL

with respect to the IP. The electron impact position is reconstructed from the energy sharing between towers or using 2 planes of silicon pads at 4 X_0 and 7.4 X_0. On one side of the IP a carefully machined tungsten mask of 17 X_0 with conical shape pointing towards the IP is placed in front of the STIC. The tungsten mask is used for defining the sharp $R_{\min}$ cut of the angular acceptance. Fig. 7 shows the STIC energy response in an electron test beam with the tungsten mask. The transition at the mask edge is very sharp. The accuracy of $R_{\min}$ defined by the tungsten conical mask is $\pm$ 20 μm, reflecting the accuracy with which the mask is surveyed and aligned. Since the mask is on one side only, the longitudinal displacements of the IP along the beam line enter as a direct correction in the measured luminosity. The IP position is measured fill-by-fill (Fig. 8) from the acollinearity and acoplanarity of non radiative Bhabha events, and cross checked with the information from the DELPHI microvertex detector. The full list of experimental systematic errors in the DELPHI luminosity measurement is reported in Table V [6].

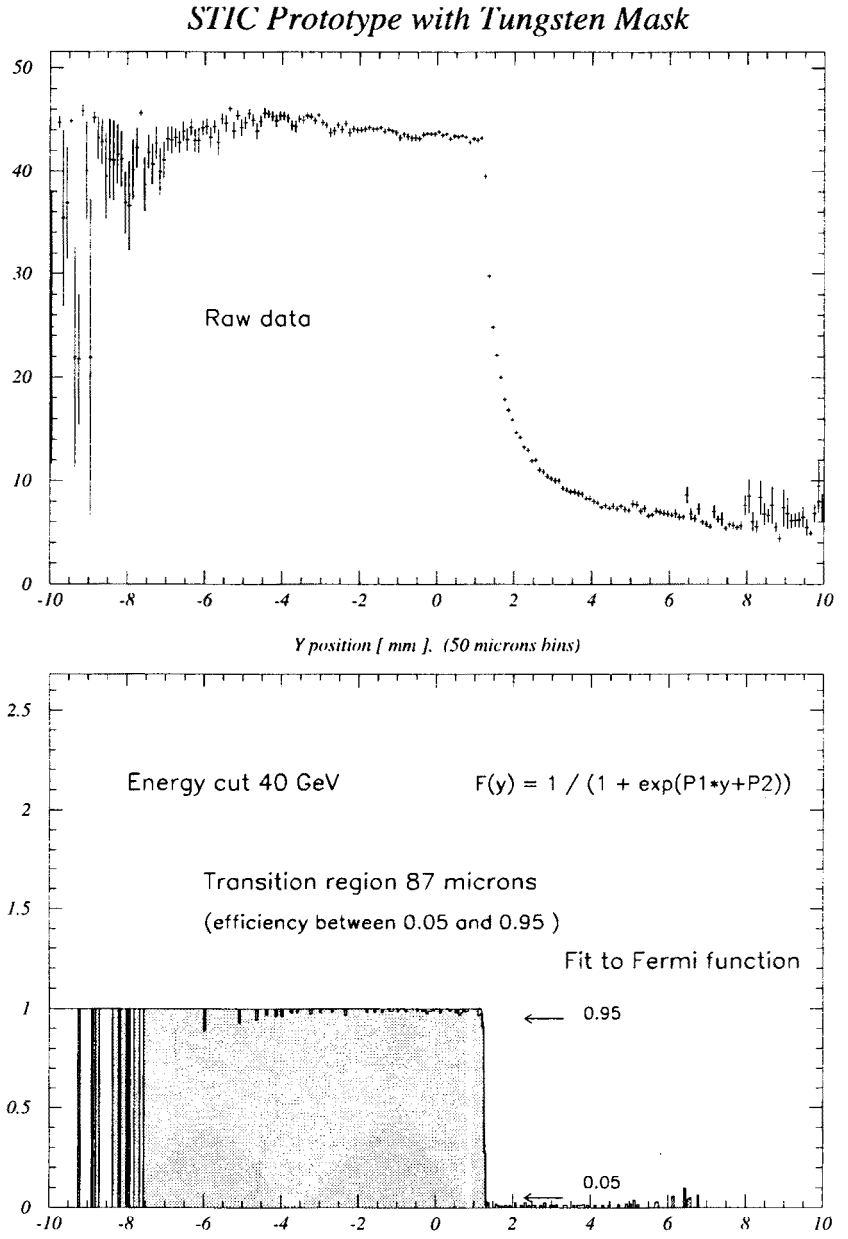
STIC Prototype with Tungsten Mask
Raw data
Y position [mm]. (50 microns bins)
Energy cut 40 GeV
F(y) = 1 / (1 + exp(P1*y+P2))
Transition region 87 microns
(efficiency between 0.05 and 0.95)
Fit to Fermi function
0.95
0.05

Fig. 7. DELPHI

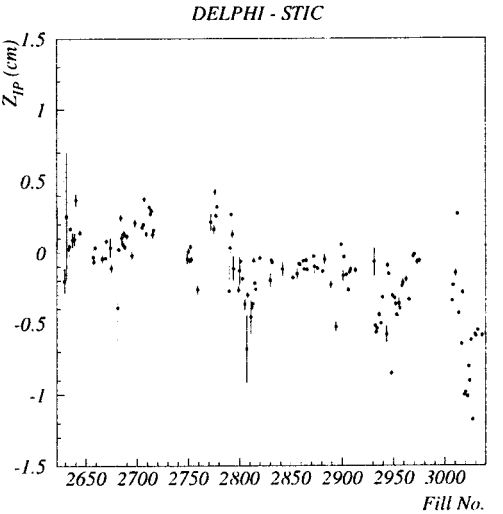

Fig. 8. DELPHI

TABLE V

DELPHI preliminary [6]

Table of Systematic Errors

Source of systematics	Contribution to $\frac{\Delta\mathcal{L}}{\mathcal{L}}$
IP position	$= 6 \times 10^{-4}$
Mask technique	$= 4 \times 10^{-4}$
MC statistics	$= 3 \times 10^{-4}$
R_A^{in} cut	$= 2 \times 10^{-4}$
R^{out} cut	$= 2 \times 10^{-4}$
Acoplanarity cut	$= 1 \times 10^{-4}$
Energy cut	$= 3 \times 10^{-4}$
Background subtraction	$= 2 \times 10^{-4}$
Trigger inefficiency	$= 2 \times 10^{-4}$
Total experimental	$= 0.9 \times 10^{-3}$
Total theoretical	$= 1.1 \times 10^{-3}$

Source of systematics	Contribution to $\frac{\Delta\mathcal{L}}{\mathcal{L}}$
distance STIC modules	$= 2 \times 10^{-4}$
temperature effects	$= 2 \times 10^{-4}$
δz_{IP} (mechanics)	$= 3 \times 10^{-4}$
δz_{IP} (reconstruction)	$= 4 \times 10^{-4}$
IP position	$= 6 \times 10^{-4}$

In the L3 detector, luminosity Bhabha events are tagged by two small-angle calorimeters placed on opposite sides of the IP. Each calorimeter [8] is an ensemble of BGO crystals (24 X_0 long) with the layout shown in Fig. 9, and it is preceded by a silicon tracker.

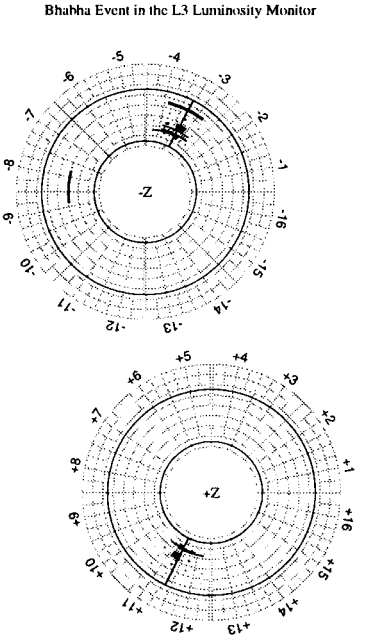

Fig. 9. L3

The silicon tracker [8] has three planes of silicon strip detectors: two planes for the R coordinate; one plane for the ϕ coordinate. For maximizing the quality of the silicon tracker coordinate the beam pipe on one side of the IP has been redesigned ("flared" beam pipe): a Bhabha electron only transverses 0.05 X_0 before reaching the tracker. The tracker coordinate is also used for realigning the BGO calorimeter. The global alignment error on $R_{\min}$ is ± 6 μm. The BGO calorimeter has an excellent energy resolution ($\sigma_E = 1.3\%$ at 45 GeV), which permits to isolate and study clean samples of radiative events. In a sample of Bhabha events with three detected electromagnetic clusters, truly radiative events are selected by checking whether the sum of the energies of the two clusters on the same side is consistent with the beam energy. In Fig. 10 one observes that such a radiative sample is well separated from the background of events where the third cluster is due to an accidental off-momentum beam electron. In the radiative event sample so selected, the dominant contribution comes from events where the photons are radiated

from the final state electrons. Assuming that the radiated photon cluster is the one with smaller energy, the photon energy spectrum is measured (Fig. 11).

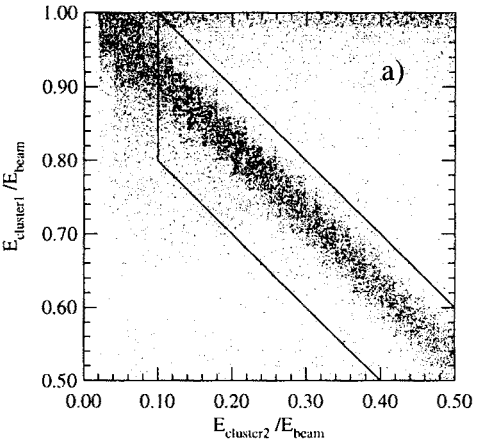

Fig. 10. L3

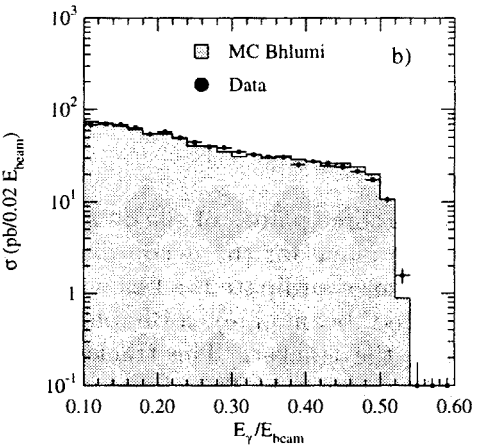

Fig. 11. L3

Comparison with the BHLUMI prediction shows very good agreement. A sample of radiative Bhabha events, in which the photons are radiated along the beam line and remain undetected, is selected by asking that the measured cluster energy on one side of the IP is smaller than 0.9 of $E_{\rm beam}$ and that there is no missing transverse momentum, which means that for the two

observed cluster the E_{e+}/E_{e-} ratio is consistent with the θ_{e-}/θ_{e+} ratio. Fig. 12 shows that the agreement between data and BHLUMI for the photon energy spectrum is excellent. In this sample the dominant contribution comes from events where the photons are radiated from the initial state electrons. The full list of experimental systematic errors in the L3 luminosity measurement is reported in Table VI [8].

TABLE VI

L3 preliminary [8]

Source	Contribution to $\Delta\mathcal{L}/\mathcal{L}$ (%)		
	BGO Analysis	BGO+Silicon Analysis	
		1993	1994
Trigger	Negligible	Negligible	Negligible
Event Selection	0.3	0.04	0.05
Background	Negligible	Negligible	Negligible
Geometry	0.4	0.06	0.03
Total Experimental	0.5	0.08	0.05
Monte Carlo Statistics	0.06	0.06	
Theory	0.11	0.11	
Total	0.5	0.15	0.14

Table 1: Systematic uncertainties on the luminosity measurement.

	1993		1994	
	Variation	Error	Variation	Error
Wafer position	$\pm 6\ \mu m$	0.015%	$\pm 6\ \mu m$	0.015%
Temperature effects	$\pm 5^{\circ}C$	0.014%	$\pm 5^{\circ}C$	0.014%
z distance	$\pm 1.6\ mm$	0.060%	$\pm 0.4\ mm$	0.016%
Total geometry		0.063%		0.026%

Table 2: The contributions of the uncertainty in the detector geometry to the systematic error.

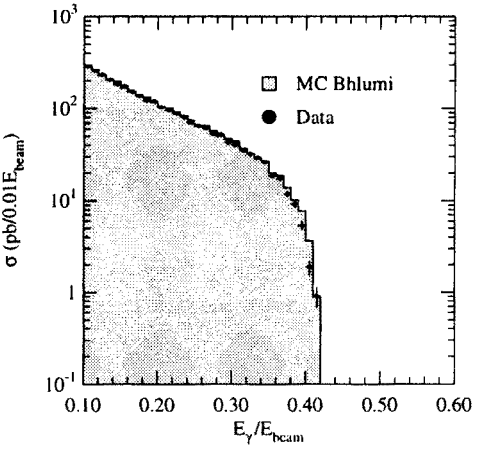

Fig. 12. L3

The ALEPH luminometer [2] was the first high-precision luminometer to be installed in a LEP experiment. Luminosity Bhabha events are tagged by two small-angle silicon-tungsten sandwich calorimeters located on opposite sides of the IP. Each calorimeter has 12 layers of 1.95 X_0 tungsten plates interleaved with silicon pad detectors. Each silicon detector layer is divided in 16 azimuthal wedges and each wedge has one 32-pad silicon detector. Each pad extends over the whole wedge in azimuth and has a radial width of 5.225 mm. The Moliere radius for 45 GeV electron showers in tungsten is about 10 mm. The detector internal alignment is measured with an uncertainty of 9 μm. The radial fiducial acceptance cut is put at the pad boundary between the third and the fourth row pad from the inner edge. For deciding whether an event at the edge of the acceptance falls in or out of it, the asymmetry A_r is used: $A_r = (E_{\rm in} - E_{\rm out})/(E_{\rm in} + E_{\rm out})$, where $E_{\rm in}$ ($E_{\rm out}$) is the energy deposited in two adjacent pads of the fourth (third) row, summed over the two layers at 6 X_0 and 8 X_0 (near the shower maximum). The event is accepted when $A_r > 0$. Fig. 13 shows the A_r dependence on the cluster radial position near the pad 3–4 boundary. The radial uncertainty on the cut based on A_r is estimated to be < 20 μm. A potential bias comes from the curvature of the pads, as discussed for the OPAL detector: the net radial offset is estimated to be $8 \pm 4 \mu$m. Events passing the angular acceptance cut are counted as luminosity Bhabha events if the energy sum $(E_{e^+} + E_{e^-})/2$ exceeds a fiducial value (typically 0.6 $E_{\rm beam}$). The estimate of how much background from accidental coincidences of off-momentum beam particles contaminates the luminosity event sample depends on the level of understanding of the background distribution. In Fig. 14 the $\Delta\phi$ between scat-

tered e^+ and e^- is plotted for events below the energy sum cut and it is compared to the estimated background distribution using artificial events constructed by mixing single-arm triggers. Except for the peak at 180° due to doubly radiative Bhabha events, the agreement is excellent. The full list of experimental systematic errors in the ALEPH luminosity measurement is reported in Table VII [3].

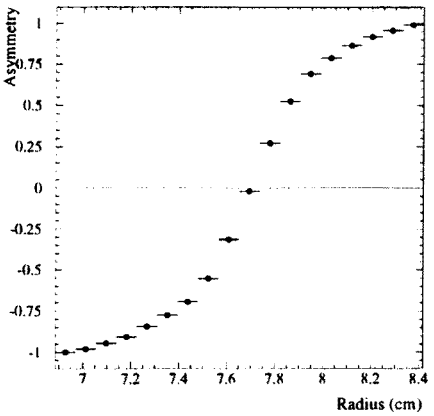

Fig. 13. ALEPH

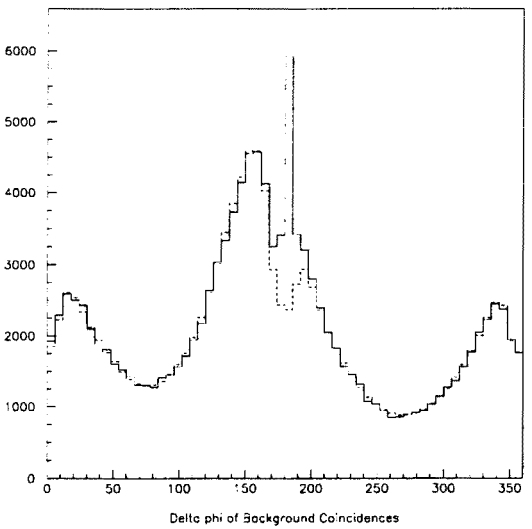

Fig. 14. ALEPH

TABLE VII

ALEPH preliminary [3]

Summary of absolute luminosity measurement systematics. The 1995 numbers labelled with * need final cross check.

Source of uncertainty	1992 SICAL Period	1993 EW Selection	1994 EW Selection	1995 EW Selection
Trigger efficiency	0.0010%	0.0002%	0.0006%	0.003%
Background estimation:				
- Off momentum e^+ or e^-	0.018%	0.003%	0.0007%	0.0009%
- Physics sources	0.010%	0.010%	0.010%	0.010%
Reconstruction efficiency	0.001%	0.001%	0.001%	0.001%
Event migration from overlays	< 0.005%	nil	0.008%	0.008% *
Absolute radial fiducial boundary:				
- Mechanical precision	0.058%	0.029%	0.029%	0.029%
- Beam and module alignments	0.035%	0.030%	0.031%	0.030%
- z position of modules	0.035%	0.035%	0.035%	0.035%
- Asymmetry precision	0.044%	0.025%	0.030%	0.030% *
- Simulation precision	0.023%	0.016%	0.016%	0.016%
Energy cuts	0.015%	0.004%	0.015%	0.040% *
Acoplanarity cut	0.005%	0.005%	0.005%	0.005%
Box cut related sources:				
- following wagon contamination				0.0006%
- preceding wagon contamination				0.001%
SUBTOTAL	0.095%	0.063%	0.069%	0.077%
Simulation statistics	0.120%	0.060%	0.024%	0.060%
TOTAL experimental error	0.153%	0.087%	0.073%	0.097%

In summary, the LEP collaborations ALEPH, DELPHI, L3 and OPAL have built and successfully operated high-tech luminometers (references [1] to [11]). An experimental uncertainty smaller than 0.1% on the luminosity measurement has been achieved by all four experiments. A very precise luminosity determination is important in order to make optimal use of the large statistics of Zs collected at LEP1, in particular for the measurement of $\Gamma_{\rm inv}/\Gamma_{\rm lept}$, one of the most stringent tests of the Standard Model at the Z peak.

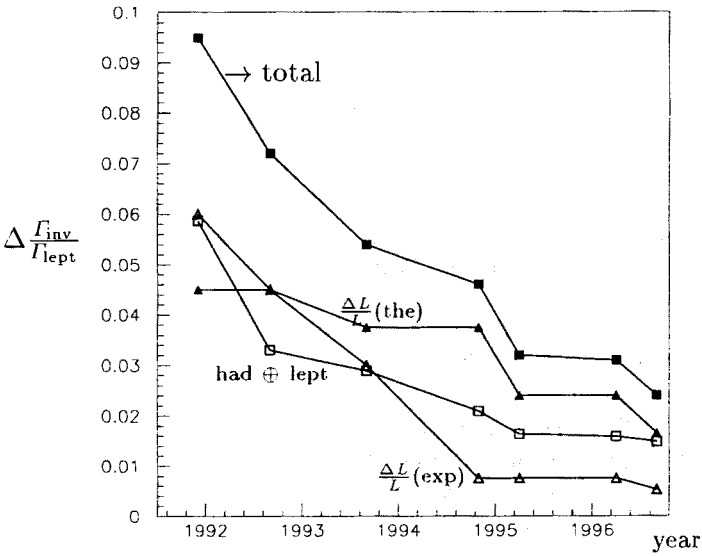

Fig. 15.

It is now appropriate to make a comment on the theoretical contribution to the luminosity uncertainty. Although the theoretical uncertainty on small-angle Bhabha scattering, currently at 0.11% [15], is nowadays adequate for each single LEP experiment, it becomes the dominant contribution to $\Delta\Gamma_{\rm inv}/\Gamma_{\rm lept}$ when combining the measurements of all four LEP experiments. Fig. 15 shows the LEP combined values of $\Delta\Gamma_{\rm inv}/\Gamma_{\rm lept}$ as they appear in the reports of the Lep ElectroWeak Working Group [13] as function of the year. The total error has been broken in its several components: the contribution from hadronic and leptonic decays of the Z (statistical and systematic), the luminosity experimental uncertainty and the luminosity theoretical uncertainty. It is clear that further improvement on the theoretical uncertainty is important.

I am indebted to my colleagues and friends in the OPAL luminosity group, to B. Bloch-Devaux of the ALEPH collaboration, to F. Filthaut of the L3 collaboration, to M. Paganoni and M. Bigi of the DELPHI collaboration. Many thanks to S. Jadach and collaborators for the excellent organization of this very successful meeting in Cracow.

REFERENCES

[1] ALEPH Collaboration, A Proposal for a Low-Angle Lminosity Calorimeter for ALEPH: SiCAL , ALEPH Note 90-8, CERN/LEPC/90-3.

[2] D. Bédérède *et al.*, Nucl. Instr. and Meth. A 365 (1995) 177.

[3] ALEPH Collaboration, Preliminary Results on Z Production Cross Section and Lepton Forward-Backward Asymmetries using the 1990-1995 Data , contributed paper to ICHEP96, Warsaw, 25-31 July 1996, PA-07-069, and references therein.

[4] The DELPHI Collaboration, Proposal to replace the Small Angle calorimeter of DELPHI, CERN/LEPC/92-6, LEPC/P2-Add.1, June 1992.

[5] A. Benvenuti *et al.*, IEEE Trans. on Nucl. Sci. 40 (1993) 537 and CERN-PPE/92-212, 11 December 1992.

[6] DELPHI Collaboration, Delphi Results on the Z Resonance Parameters and Measurement of Fermion-Pair Production at LEP1.5 Energies for the Summer 1996 Conferences, DELPHI Note 96-118 CONF 65 and contributed paper to ICHEP96, Warsaw, 25-31 July 1996, PA-07-001, and references therein; DELPHI Collaboration, Performance of the new high precision luminosity monitor of DELPHI at LEP, contributed paper to EPS-HEP-95 Brussels, 27th July-2nd August 1995, ref. eps0528, and DELPHI Note 95-68 PHIS 503, 30 June 1995.

[7] L3 Collaboration, L3 Report to LEPC , CERN/LEPC/92-6, June 1992.

[8] I.C. Brock *et al.*, Luminosity Measurement in the L3 Detector at LEP, preprint CERN-PPE/96-089, submitted to *Nucl. Instrum. Methods Phys. Res.* **A**.

[9] The OPAL Collaboration, Proposal for Upgrading the OPAL Luminosity Detector, CERN/LEPC/91-8, LEPC/M-100, October 1991.

[10] B.E. Anderson *et al.*, *IEEE Trans. on Nucl. Sci.* **41**, 845 (1994).

[11] OPAL Collaboration, A Preliminary Update of the Z Line Shape and Lepton Asymmetry Measurements with a Revised 1993-1994 LEP Energy and 1995 Lepton Asymmetry, OPAL Physics Note PN242, July 1996, and references therein; The OPAL Collaboration, A Preliminary Update of the Z Line Shape and Lepton Asymmetry Measurements with the 1993-1994 Data , contributed paper to EPS-HEP-95 Brussels, 27th July-2nd August 1995, ref. eps0292, and OPAL Physics Note PN166, 27 February 1995.

[12] CDF Collaboration, J. Lys, talk at ICHEP96, Warsaw, 25-31 July 1996, to appear in the proceedings; DØ Collaboration, S. Protopopescu, talk at ICHEP96, Warsaw, 25-31 July 1996, to appear in the proceedings; P. Tipton, talk at ICHEP96, Warsaw, 25-31 July 1996, to appear in the proceedings.

[13] M. Pepe Altarelli, *Acta Phys. Pol.* **B28**, this issue; A Combination of Preliminary LEP and SLD Electroweak Measurements and Constraints on the Standard Model, LEPEWWG Internal Note 96-02, ALEPH 96-107 PHYSIC 96-98, DELPHI 96-121 PHYS 631, L3 Note 1975, OPAL Technical Note TN 399, SLD Physics Note 52.

[14] D. Bardin *et al.*, *Z. Phys.* **C44**, 493 (1989); *Comp. Phys. Comm.* **59**, 303 (1990); *Nucl. Phys.* **B351**, 1 (1991); *Phys. Lett.* **B255**, 290 (1991); CERN-TH 6443/92 (May 1992).

[15] Event Generators for Bhabha Scattering, by S. Jadach (convener), O. Nicrosini (convener), H. Anlauf, A. Arbuzov, M. Bigi, H. Burkhardt, M. Cacciari, M. Caffo, H. Czyż, M. Dallavalle, J.H. Field, F. Filthaut, F. Jegerlehner, E. Kuraev, G. Montagna, T. Ohl, F. Piccinini, B. Pietrzyk, W. Płaczek, E. Remiddi, M. Skrzypek, L. Trentadue, B.F.L. Ward, Z. Wąs, in Reports of the Workshop on Physics at LEP2, eds G. Altarelli, T. Sjöstrand and F. Zwirner, CERN 96-01, vol.2; e-Print Archive: hep-ph/9602393; A. Arbuzov *et al.*, *Phys. Lett.* **B383**, 238 (1996).

[16] B.F.L. Ward's *Acta Phys. Pol.* **B** this issue; N. Merenkov's *Acta Phys. Pol.* **B** this issue.

[17] BHLUMI V4.03 : S. Jadach, E. Richter Wąs, B.F.L. Ward and Z. Wąs, *Phys. Lett.* **B353**, 362 (1995); S. Jadach, W. Płaczek, B.F.L. Ward, *Phys. Lett.* **B353**, 349 (1995).

[18] M. Böhm, A. Denner, W. Hollik, *Nucl. Phys.* **B304**, 687 (1988); F.A. Berends, R. Kleiss, W. Hollik, *Nucl. Phys.* **B304**, 712 (1988).